

PCCP

Accepted Manuscript



This is an *Accepted Manuscript*, which has been through the Royal Society of Chemistry peer review process and has been accepted for publication.

Accepted Manuscripts are published online shortly after acceptance, before technical editing, formatting and proof reading. Using this free service, authors can make their results available to the community, in citable form, before we publish the edited article. We will replace this *Accepted Manuscript* with the edited and formatted *Advance Article* as soon as it is available.

You can find more information about *Accepted Manuscripts* in the [Information for Authors](#).

Please note that technical editing may introduce minor changes to the text and/or graphics, which may alter content. The journal's standard [Terms & Conditions](#) and the [Ethical guidelines](#) still apply. In no event shall the Royal Society of Chemistry be held responsible for any errors or omissions in this *Accepted Manuscript* or any consequences arising from the use of any information it contains.

Can HN=NH, FN=NH, or HN=CHOH Bridge the σ -Hole and the Lone Pair at P in Binary Complexes with H₂XP, for X = F, Cl, NC, OH, CN, CCH, CH₃, and H?[%]

Janet E. Del Bene,^{*a} Ibon Alkorta,^{*b} and José Elguero^b

^a Department of Chemistry, Youngstown State University, Youngstown, Ohio 44555 USA. E-mail: jedelbene@ysu.edu

^b Instituto de Química Médica (IQM-CSIC), Juan de la Cierva, 3, E-28006 Madrid, Spain. E-mail: ibon@iqm.csic.es

[%]Electronic supplementary information (ESI) available: Geometries, total energies, and molecular graphs of all complexes; components of spin-spin coupling constants ^{1p}J(P-N), ^{2h}J(N-P), J(N-P), and ^{2h}J(O-P); plots of energy densities versus corresponding bond distances; plot of ^{2h}J(O-P) versus the O-P distance. See DOI:10.1039/XXXXXX

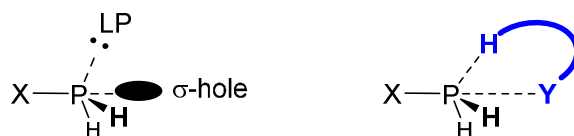
ABSTRACT

Ab initio MP2/aug'-cc-pVTZ calculations have been carried out to investigate the properties of complexes formed between H_2XP , for $X = F, Cl, NC, OH, CN, CCH, CH_3,$ and H , and the possible bridging molecules $HN=NH, FN=NH,$ and $HN=CHOH$. $H_2XP:HNNH$ and $H_2XP:FNNH$ complexes are stabilized by $P\cdots N$ pnictogen bonds, except for $H_2(CH_3)P:FNNH$ and $H_3P:FNNH$ which are stabilized by $N-H\cdots P$ hydrogen bonds. $H_2XP:HNCHOH$ complexes are stabilized by $P\cdots N$ pnictogen bonds and nonlinear $O-H\cdots P$ hydrogen bonds. For a fixed H_2XP molecule, binding energies decrease in the order $HNCHOH > HNNH > FNNH$, except for the binding energies of $H_2(CH_3)P$ and H_3P with $HNNH$ and $FNNH$. Binding energies of complexes with $HNCHOH$ and $HNNH$ increase as the $P-N_1$ distance decreases, but binding energies of complexes with $FNNH$ show little dependence on this distance. The large binding energies of $H_2XP:HNCHOH$ complexes arise from a cooperative effect involving electron-pair acceptance by P to form a pnictogen bond, and electron-pair donation by P to form a hydrogen bond. The dominant charge-transfer interaction in these complexes involves electron-pair donation by N across the pnictogen bond, except for complexes in which X is one of the more electropositive substituents, $CCH, CH_3,$ and H . For these, lone-pair donation by P across the hydrogen bond dominates. AIM and NBO data for these complexes are consistent with their bonding characteristics, showing molecular graphs with bond critical points and charge-transfer interactions associated with hydrogen and pnictogen bonds. EOM-CCSD spin-spin coupling constants $^1J(P-N)$ across the pnictogen bond for each series of complexes correlate with the $P-N$ distance. In contrast, $^2hJ(O-P)$ values for complexes $H_2XP:HNCHOH$ do not correlate with the $O-P$ distance, a consequence of the nonlinearity of these hydrogen bonds.

INTRODUCTION

Since the publication of two papers on pnictogen bonds in 2011,^{1,2} interest in this bond has grown dramatically, as evidenced not only by the number of research papers published on this subject, but also by the number of review articles which have appeared recently.^{3,4,5} The pnictogen bond is an intermolecular bond formed when a Group 15 atom acts as an electron-pair acceptor. According to Politzer and Murray,^{6,7} bond formation at the pnictogen atom occurs through the σ -hole, a positive region of the molecular electrostatic potential. In addition to the σ -hole at P, there is also a lone pair of electrons. That the phosphorus atom can act as both an electron-pair acceptor and an electron-pair donor has been documented in several studies. In a 2013 paper,⁸ we demonstrated that the phosphorus in a pnictogen-bonded complex can simultaneously act as an electron-pair donor to a Lewis acid such as HF to form a hydrogen bond, ClF to form a halogen bond, LiH to form a lithium bond, or BeH₂ to form a beryllium bond. The P atom also acts as an electron-pair donor and acceptor in pnictogen-bonded trimers (PH₂X)₃ and tetramers (PH₂X)₄.^{9,10}

In the present paper, we ask whether or not a single small molecule can interact with P at both its σ -hole and its lone pair, as illustrated in Scheme 1. For this study we have used a series of substituted H₂XP molecules, for X = F, Cl, NC, OH, CN, CCH, CH₃, and H, in order to vary the electron-accepting and electron-donating abilities of P. The three bridging molecules are HN=NH, FN=NH, and HN=CHOH (formamidic acid), which also differ in their electron-donating ability to form a pnictogen bond, and their electron accepting ability to form a hydrogen bond. Can both of these bonds exist simultaneously in these simple binary complexes, or will these complexes be stabilized by either a pnictogen bond or a hydrogen bond? The structures of these complexes, their binding energies, charge-transfer energies, and spin-spin coupling constants ¹P(P-N), ²J(N-P), and ²J(O-P), will be used to provide an answer to this question.



Scheme 1. Representation of the lone pair and the σ -hole in an isolated phosphine (left) and the potential bridging interaction (right) involving atoms Y and H, in blue color.

METHODS

The structures of the monomers H_2XP , $HN=NH$, $FN=NH$, and $HN=CHOH$ (formamidic acid), and the complexes $H_2XP:HNNH$, $H_2XP:FNNH$, and $H_2XP:HNCHOH$ were optimized at second-order Møller-Plesset perturbation theory (MP2)^{11,12,13,14} with the aug'-cc-pVTZ basis set.¹⁵ This basis set is derived from the Dunning aug-cc-pVTZ basis set^{16,17} by removing diffuse functions from hydrogen atoms. Frequencies were computed to establish that the optimized structures correspond to equilibrium structures on their potential surfaces. The binding energy of a complex is defined as the negative energy ($-\Delta E$) for the reaction which forms the complex from the isolated monomers. All calculations were performed using the Gaussian 09 program.¹⁸

The electron densities of the complexes have been analyzed using the Atoms in Molecules (AIM) methodology^{19,20,21,22} employing the AIMAll²³ program. The topological analysis of the electron density produces the molecular graph of each complex. This graph identifies the location of electron density features of interest, including the electron density (ρ) maxima associated with the various nuclei, saddle points which correspond to bond critical points (BCPs), and ring critical points which indicate a minimum electron density within a ring. The zero gradient line which connects a BCP with two nuclei is the bond path. The electron density at the BCP (ρ_{BCP}), its Laplacian ($\nabla^2\rho_{BCP}$), and the total energy density (H_{BCP}) can also be used to characterize interactions.²⁴ In addition, the Natural Bond Orbital (NBO)²⁵ method has been used to analyze the stabilizing charge-transfer interactions employing the NBO-6 program.²⁶ Since MP2 orbitals are nonexistent, the charge-transfer interactions have been computed using the B3LYP functional^{27,28} with the aug'-cc-pVTZ basis set at the MP2/aug'-cc-pVTZ complex geometries, so that at least some electron correlations effects could be included.

Spin-spin coupling constants were evaluated using the equation-of-motion coupled cluster singles and doubles (EOM-CCSD) method in the CI(configuration interaction)-like approximation,^{29,30} with all electrons correlated. For these calculations, the Ahlrichs³¹ qzp basis set was placed on ^{13}C , ^{15}N , ^{17}O , and ^{19}F , and the qz2p basis set on ^{31}P , ^{35}Cl , and hydrogen-bonded 1H atoms. The Dunning cc-pVDZ basis was placed on all other 1H atoms. The EOM-CCSD calculations were performed using ACES II³² on the IBM Cluster 1350 (Glenn) at the Ohio Supercomputer Center.

RESULTS AND DISCUSSION

The molecular electrostatic potentials on the 0.001 au electron density isosurface of the isolated phosphines show the presence of a maximum and a minimum value around the phosphorous atom associated to the σ -hole and lone pair, respectively,³³ as illustrated in Scheme 1. The monomers HNNH, FNNH, and HNCHOH may act as electron pair donors to the H₂XP molecules through the σ -hole to form P \cdots N pnicogen bonds, and also as electron-pair acceptors to form N-H \cdots P or O-H \cdots P hydrogen bonds. To distinguish between the two N-H bonds in HNNH, H₁ is bonded to the nitrogen N₁ that takes part in the pnicogen bond, and H₂ is bonded to N₂, whether or not the N₂-H₂ group is involved in a hydrogen-bonding interaction. Fig. 1 illustrates these designations in the H₂(CH₃)P:HNNH complex.

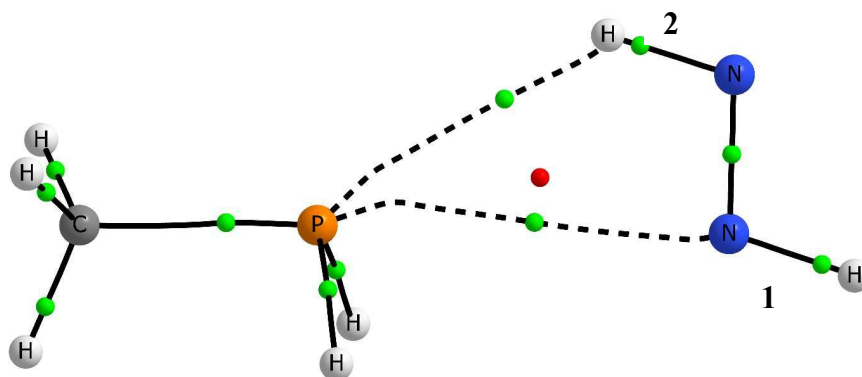


Fig. 1. The molecular graph of the H₂(CH₃)P:HNNH complex illustrating the labeling of the two N-H groups and the locations of bond critical points.

Structures, Binding Energies, Charge-Transfer Energies, and NBO Data

The structures, total energies, and molecular graphs of the complexes H₂XP:HNNH, H₂XP:FNNH, and H₂XP:HNCHOH are reported in Table S1 of the Supporting Information. The binding energies, intermolecular P-N₁ distances, and N₁-P-A angles across the pnicogen bonds are reported in Table 1, with A the atom of X that is directly bonded to P. The H₂XP molecules are listed in Table 1 according to decreasing binding energies of their complexes with HNNH. This is also the order of decreasing binding energies for complexes with HNCHOH, but not for complexes with FNNH. The binding energies range between 13 and 31 kJ mol⁻¹ for HNNH complexes and between 20 and 44 kJ mol⁻¹ for HNCHOH complexes, but exhibit a much

narrower range from 12 to 21 $\text{kJ}\cdot\text{mol}^{-1}$ for complexes with FNNH. For a fixed H_2XP molecule, binding energies decrease in the order



except for the binding energies of $\text{H}_2(\text{CH}_3)\text{P}$ and H_3P with HNNH and FNNH. The reason for this reversal will become evident in the following subsections of this paper. Fig. 2 presents a plot of these binding energies versus the P- N_1 distance. As is evident from this figure, binding

Table 1. Binding energies ($-\Delta E$, $\text{kJ}\cdot\text{mol}^{-1}$), P- N_1 distances (R, Å), and N_1 -P-A angles (\angle , $^\circ$)^a across $\text{P}\cdots\text{N}_1$ pnictogen bonds in complexes of H_2XP with HNNH, FNNH, and HNCHOH

Molecule:	HNNH		FNNH		HNCHOH	
$\text{H}_2\text{XP} =$	$-\Delta E$	$\text{R(P-N}_1) \angle$	$-\Delta E$	$\text{R(P-N}_1) \angle$	$-\Delta E$	$\text{R(P-N}_1) \angle$
H_2FP	31.3	2.512 173	18.8	2.773 174	44.4	2.507 170
H_2CIP	26.9	2.651 173	15.0	2.894 173	37.4	2.620 168
$\text{H}_2(\text{NC})\text{P}$	25.2	2.646 174	15.7	2.939 177	36.5	2.615 170
$\text{H}_2(\text{OH})\text{P}$	21.4	2.755 174	16.6	3.054 179	33.0	2.778 169
$\text{H}_2(\text{CN})\text{P}$	19.7	2.882 173	12.0	3.071 176	27.1	2.874 167
$\text{H}_2(\text{CCH})\text{P}$	17.0	3.009 176	15.2	3.293 172	25.2	3.021 170
$\text{H}_2(\text{CH}_3)\text{P}$	14.4	3.210 179	20.9	4.013 140	23.8	3.211 172
H_3P	13.1	3.189 176	15.9	3.974 145	20.1	3.211 169

a) A is the atom of X that is directly bonded to P.

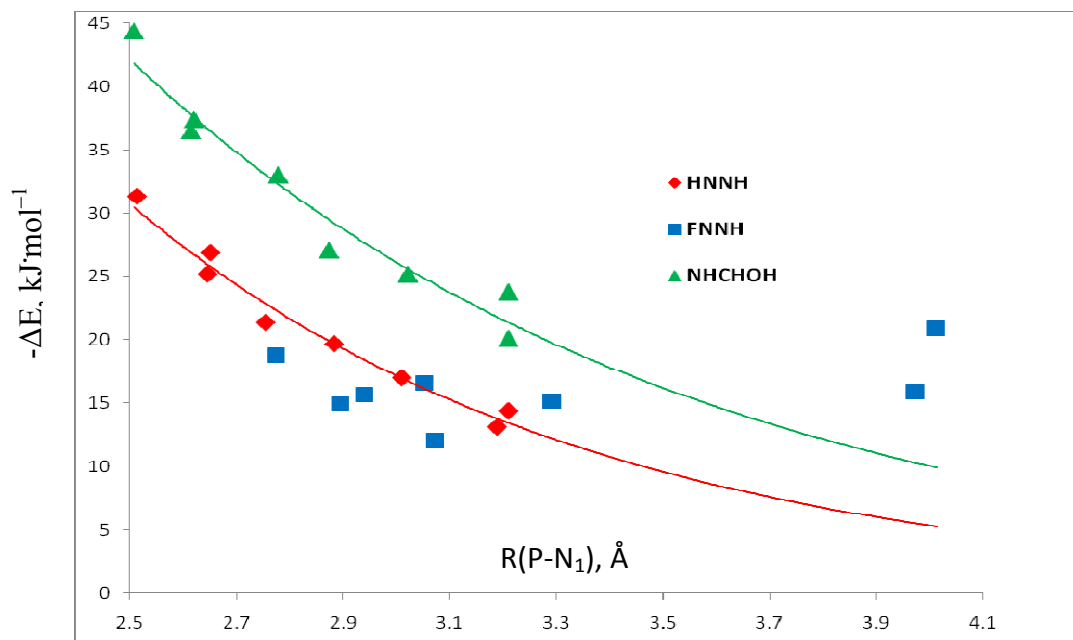


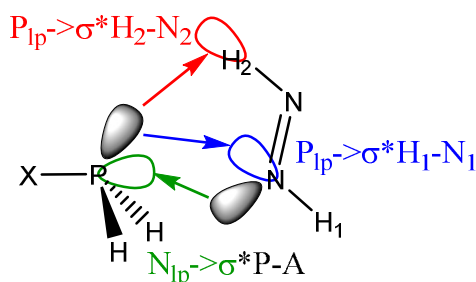
Fig. 2. Binding energies ($-\Delta E$) versus the P-N_1 distance across the pnicoen bond for complexes of H_2XP with HNNH, FNNH, and HNCHOH

energies of $\text{H}_2\text{XP}:\text{HNNH}$ and $\text{H}_2\text{XP}:\text{HNCHOH}$ complexes increase exponentially as the intermolecular P-N_1 distance decreases, with correlation coefficients of 0.977 and 0.944, respectively. In contrast, the binding energies of the $\text{H}_2\text{XP}:\text{FNNH}$ complexes show little dependence on the P-N_1 distance. Among the complexes with FNNH, $\text{H}_2(\text{CH}_3)\text{P}:\text{FNNH}$ and $\text{H}_3\text{P}:\text{FNNH}$ have the longest P-N_1 distances, but relatively large binding energies of 21 and 16 kJ mol^{-1} , respectively. In order to understand these relationships, it is necessary to examine the structures of these complexes and the charge-transfer interactions which contribute to their stabilization.

Complexes with HNNH. The molecule HNNH may act as an electron-pair donor to form a $\text{P}\cdots\text{N}_1$ pnicoen bond, or a proton donor to form a $\text{N}_2\text{-H}_2\cdots\text{P}$ hydrogen bond. That the binding energies of $\text{H}_2\text{XP}:\text{HNNH}$ complexes correlate with the P-N_1 distance is a strong indication that the pnicoen bond is by far the dominant interaction stabilizing these complexes. The values of the $\text{N}_1\text{-P-A}$ angles which are reported in Table 1 vary from 173 to 179°, indicating that these three atoms approach a linear arrangement, as expected for complexes stabilized by pnicoen bonds. The question that remains is whether $\text{N}_2\text{-H}_2\cdots\text{P}$ hydrogen bonds exist in these complexes, and if so, what role do they play in stabilization? Some insight into the answer to

this question may be found from the data of Table 2, which reports values of the H_2-N_2-P angles. These angles vary between 51 and 59° for all complexes except $H_2(CCH)P:HNNH$, $H_2(CH_3)P:HNNH$, and $H_3P:HNNH$. Since binding energies of complexes with $X-H\cdots Y$ hydrogen bonds decrease as the hydrogen bond becomes nonlinear, $H-X-Y$ angles greater than about 30° suggest that hydrogen bonds are very weak or essentially nonexistent in these complexes. As the substituent X becomes more electropositive, the H_2-N_2-P angle decreases to 45 , 38 , and 40° in $H_2(CCH)P:HNNH$, $H_2(CH_3)P:HNNH$, and $H_3P:HNNH$, respectively. The interaction between P and H_2-N_2 may have some significance, even though the hydrogen bond is still nonlinear and weak.

The charge-transfer interactions in complexes $H_2XP:HNNH$ are depicted in Scheme 2. The charge-transfer energies which are reported in Table 3 are consistent with the description of the bonding in these complexes given above. In all complexes except $H_2(CH_3)P:HNNH$, the dominant charge-transfer interaction occurs across the pnictogen bond from the nitrogen lone pair to the antibonding σ^* P-A orbital. There is also a second much weaker charge-transfer interaction across the pnictogen bond, with electron donation from P to the σ^* N_1-H_1 orbital. The third charge-transfer interaction occurs across the $N_2-H_2\cdots P$ hydrogen bond. The $P_{lp}\rightarrow\sigma^*H_2-N_2$ charge-transfer energy is greatest in complexes $H_2(CCH)P:HNNH$, $H_2(CH_3)P:HNNH$, and $H_3P:HNNH$ which have the more electropositive substituents. However, only in the $H_2(CH_3)P:HNNH$ complex is the $P_{lp}\rightarrow\sigma^*H_2-N_2$ charge-transfer energy greater than the $N_{lp}\rightarrow\sigma^*P-A$ energy, but it is still only 9 kJ mol^{-1} .



Scheme 2. Representation of the charge-transfer interactions $P_{lp}\rightarrow\sigma^*H_2-N_2$ across the $N_2-H_2\cdots P$ hydrogen bond and $N_{lp}\rightarrow\sigma^*P-A$ and $P_{lp}\rightarrow\sigma^*N_1-H_1$ across the $P\cdots N$ pnictogen bond

The molecular graphs of the complexes illustrated in Fig. 1 and Fig. S1 of the Supporting Information exhibit a single intermolecular $P\cdots N$ BCP except in complexes with $X = CCH, CH_3$ and H . For these, there is a second BCP associated with the $N_2-H_2\cdots P$ hydrogen bonds. The electron densities at the $P\cdots N$ BCPs reported in Table S2 have values between 0.009 au for the $H_2(CH_3)P:HNNH$ complex with the longest P-N distance, to 0.035 au for the $H_2FP:HNNH$ complex which has the shortest P-N distance. The Laplacians are always positive, but the total energy densities are negative for the complexes with $X = F, Cl, OH,$ and $NC,$ which indicates that these $P\cdots N$ bonds have some covalent character. For the three cases with a BCP associated with the $N_2-H_2\cdots P$ hydrogen bonds, ρ_{BCP} values are 0.01 au and both the Laplacians and the energy densities are positive.

Table 2. The Y_2-P and H_2-P distances (R, Å), and H_2-Y_2-P angles (\angle , °) in complexes of H_2XP with HNNH, FNNH, and HNCHOH^a

Molecule:	HNNH		FNNH		HNCHOH	
$H_2XP=$	$R(N_2-P) <$	$R(H_2-P)$	$R(N_2-P) <$	$R(H_2-P)$	$R(O-P) <$	$R(H_2-P)$
H_2FP	3.204 59	2.809	3.475 57	3.040	3.218 27	2.386
H_2ClP	3.298 57	2.864	3.599 57	3.165	3.332 28	2.506
$H_2(NC)P$	3.296 57	2.862	3.526 51	2.988	3.282 26	2.442
$H_2(OH)P$	3.328 52	2.819	3.473 42	2.799	3.271 21	2.383
$H_2(CN)P$	3.420 51	2.887	3.632 50	3.070	3.432 23	2.564
$H_2(CCH)P$	3.432 45	2.804	3.534 34	2.739	3.364 18	2.451
$H_2(CH_3)P$	3.473 38	2.729	3.559 0	2.520	3.321 12	2.371
H_3P	3.492 40	2.776	3.615 5	2.586	3.377 13	2.435

a) Y is N_2 of HNNH and FNNH, and O bonded to H_2 in HNCHOH.

Table 3. Charge-transfer energies ($\text{kJ}\cdot\text{mol}^{-1}$) across pnictogen bonds and possible hydrogen bonds in complexes of H_2XP with HNNH, FNNH, and HNCHOH

	ZB ^a	ZB ^b	HB ^c
HNNH: H_2XP			
$\text{H}_2\text{XP} =$	$\text{N}_{\text{lp}} \rightarrow \sigma^* \text{P-A}$	$\text{P}_{\text{lp}} \rightarrow \sigma^* \text{N}_1\text{-H}_1$	$\text{P}_{\text{lp}} \rightarrow \sigma^* \text{H}_2\text{-N}_2$
H_2FP	58.3	8.4	4.3
H_2ClP	45.1	5.4	3.1
$\text{H}_2(\text{NC})\text{P}$	45.3	5.6	3.3
$\text{H}_2(\text{OH})\text{P}$	28.3	4.6	4.7
$\text{H}_2(\text{CN})\text{P}$	21.4	2.9	3.2
$\text{H}_2(\text{CCH})\text{P}$	13.7	2.2	5.4
$\text{H}_2(\text{CH}_3)\text{P}$	6.3	1.2	9.0
H_3P	8.1	1.3	6.7
FNNH: H_2XP			
$\text{H}_2\text{XP} =$	$\text{N}_{\text{lp}} \rightarrow \sigma^* \text{P-A}$	$\text{P}_{\text{lp}} \rightarrow \sigma^* \text{N}_1\text{-F}$	$\text{P}_{\text{lp}} \rightarrow \sigma^* \text{H}_2\text{-N}_2$
H_2FP	24.0	5.9	2.2
H_2ClP	15.5	3.5	2.7
$\text{H}_2(\text{NC})\text{P}$	20.1	3.6	1.4
$\text{H}_2(\text{OH})\text{P}$	9.2	2.7	7.7
$\text{H}_2(\text{CN})\text{P}$	10.9	2.4	2.3
$\text{H}_2(\text{CCH})\text{P}$	4.5	1.3	11.0
$\text{H}_2(\text{CH}_3)\text{P}$			35.9
H_3P			25.7
HNCHOH: H_2XP			
$\text{H}_2\text{XP} =$	$\text{N}_{\text{lp}} \rightarrow \sigma^* \text{P-A}$		$\text{P}_{\text{lp}} \rightarrow \sigma^* \text{H}_2\text{-O}$
H_2FP	65.6		38.9
H_2ClP	56.7		26.9
$\text{H}_2(\text{NC})\text{P}$	55.0		22.0
$\text{H}_2(\text{OH})\text{P}$	29.8		43.8
$\text{H}_2(\text{CN})\text{P}$	25.1		17.9
$\text{H}_2(\text{CCH})\text{P}$	15.4		32.3
$\text{H}_2(\text{CH}_3)\text{P}$	7.6		49.3
H_3P	8.8		35.3

a) $\text{N}_{\text{lp}} \rightarrow \sigma^* \text{P-A}$ refers to charge transfer across the pnictogen bond from N_1 to the antibonding P-A orbital of H_2XP , with A the atom of X directly bonded to P.

b) $\text{P}_{\text{lp}} \rightarrow \sigma^* \text{N}_1\text{-H}_1$ and $\text{P}_{\text{lp}} \rightarrow \sigma^* \text{N}_1\text{-F}$ refer to charge transfer across the pnictogen bond from P to the antibonding $\text{N}_1\text{-H}_1$ orbital of HNNH, and the antibonding $\text{N}_1\text{-F}$ orbital of FNNH.

c) $\text{P}_{\text{lp}} \rightarrow \sigma^* \text{H}_2\text{-N}_2$ and $\text{P}_{\text{lp}} \rightarrow \sigma^* \text{H}_2\text{-O}$ refer to charge transfer from P to the possible proton donor $\text{N}_2\text{-H}_2$ of HNNH and FNNH, and O-H_2 of HNCHOH.

Complexes with FNNH. The replacement of H by F makes FNNH a poorer electron-pair donor through N_1 than HNNH for the $P \cdots N$ pnictogen bond. This is evident from the reduced binding energies and the longer P- N_1 distances reported in Table 1 for complexes of FNNH with H_2XP when X is one of the more electronegative substituents F, Cl, NC, OH, and CN. When X is one of the more electropositive groups, the bonding picture begins to change. Although the P-N distance of 3.293 Å in $H_2(CCH)P:FNNH$ is longer than the distance of 3.009 Å in $H_2(CCH)P:HNNH$, the binding energies of these two complexes are similar at 15 and 17 $\text{kJ}\cdot\text{mol}^{-1}$, which suggests that the $N_2-H_2 \cdots P$ hydrogen bond may have increased importance. This is also suggested by the reduced value of 34° for the H_2-N_2-P angle, and the increase in the P- N_1 distance. This distance increases further to 4.013 and 3.974 Å in $H_2(CH_3)P:FNNH$ and $H_3P:FNNH$, yet these two complexes have relatively large binding energies of 21 and 16 $\text{kJ}\cdot\text{mol}^{-1}$, respectively. There is no pnictogen bond in these two complexes, but rather $N_2-H_2 \cdots P$ hydrogen bonds, as illustrated in Fig. 3 for $H_2(CH_3)P:FNNH$. In the $H_2(CH_3)P:FNNH$ and $H_3P:FNNH$ complexes, the H_2-P distances are short and the hydrogen bonds are linear, with H_2-N_2-P angles of 0° and 5° , respectively. It is not surprising that no correlation is seen in Fig. 2 between the binding energies of $H_2XP:FNNH$ complexes and the P- N_1 distance across the pnictogen bond.

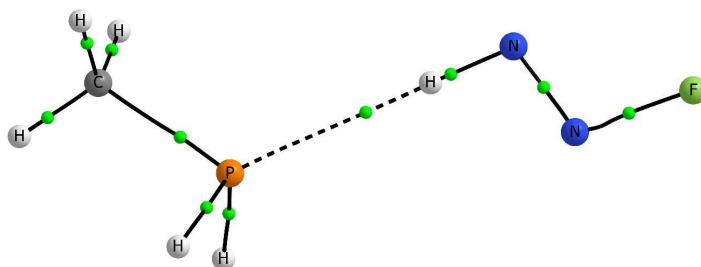


Fig. 3. Molecular graph of $H_2(CH_3)P:FNNH$ with a linear $N_2-H_2 \cdots P$ hydrogen bond.

That the pnictogen bond in the complexes with FNNH is weaker than the pnictogen bond in HNNH complexes can be inferred from the reduced values of the $N_{1p} \rightarrow \sigma^*P-A$ and $P_{1p} \rightarrow \sigma^*N-F$ charge-transfer energies in the Table 3. Moreover, the large values of the H_2-N_2-P angles and the small $P_{1p} \rightarrow \sigma^*H_2-N_2$ charge-transfer energies are indicative of very weak $N_2-H_2 \cdots P$ interactions in complexes $H_2XP:FNNH$ when X is one of the more electronegative substituents. However, in the complex $H_2(CCH)P:FNNH$, the $P_{1p} \rightarrow \sigma^*H_2-N_2$ charge-transfer energy increases to 11 $\text{kJ}\cdot\text{mol}^{-1}$

¹, which is greater than the charge-transfer energies across the pnictogen bond in this complex. These changes are even more pronounced in the complexes $H_2(CH_3)P:FNNH$ and $H_3P:FNNH$ which have $P_{1p} \rightarrow \sigma^*H_2-N_2$ charge-transfer energies of 36 and 26 $\text{kJ}\cdot\text{mol}^{-1}$, respectively, and $N_{1p} \rightarrow \sigma^*P-A$ and $P_{1p} \rightarrow \sigma^*N_1-F$ charge-transfer energies which are less than 1 $\text{kJ}\cdot\text{mol}^{-1}$. Thus, these latter two complexes are stabilized solely by $N_2-H_2 \cdots P$ hydrogen bonds.

The molecular graphs of these complexes are illustrated in Table S1 of the Supporting Information. These graphs exhibit only one BCP for the more electronegative X groups, except for the $H_2(OH)P:FNNH$ which also has a BCP corresponding to the $N_2-H_2 \cdots P$ hydrogen bond. Complexes with the more electropositive groups CCH, CH_3 and H have only one BCP associated with the $N_2-H_2 \cdots P$ hydrogen bond. Electron densities at $P \cdots N$ BCPs are less than those of the corresponding $H_2XP:HNNH$ complexes. The values of $\nabla^2\rho_{BCP}$ and H_{BCP} are always positive. In contrast, electron densities at BCPs for the $N_2-H_2 \cdots P$ hydrogen bonds range from 0.01 to 0.02 au for the complexes with X = OH, CCH, CH_3 , and H. The Laplacians and total energy densities are positive except for the complexes with X = H and CH_3 , which have very small but negative values of the energy densities.

Complexes with HNCHOH. HNCHOH should have an electron-pair donating strength similar to that of HNNH, but it should also be a better proton donor through the O-H group. Table 1 shows that the binding energy of a given $H_2XP:HNCHOH$ complex is at least 7 $\text{kJ}\cdot\text{mol}^{-1}$ greater than the binding energy of the corresponding complex with HNNH. Fig. 2 shows that the binding energies of $H_2XP:HNCHOH$ complexes increase exponentially as the P-N distance decreases, with a correlation coefficient of 0.944. Moreover, at any given distance, the binding energy of an $H_2XP:HNCHOH$ complex is greater than that of an $H_2XP:HNNH$ complex, which suggests that the $P \cdots N$ pnictogen bond is also stronger. Nevertheless, part of the increase in the binding energies of HNCHOH complexes is due to the approach to linearity of the $O-H_2 \cdots P$ hydrogen bond, with H_2-O-P angles between 12 and 28°. The structure of $H_2(CN)P:HNCHOH$ is illustrated in Fig. 4.

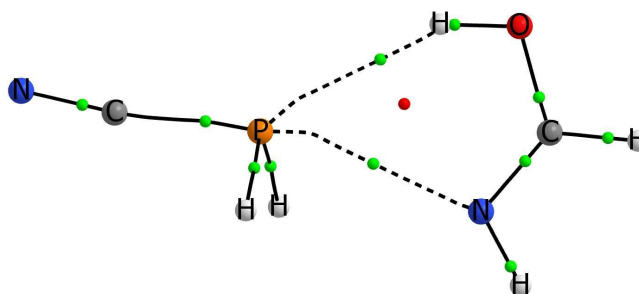


Fig. 4. Molecular graph of $\text{H}_2(\text{CN})\text{P}:\text{HNCHOH}$ illustrating the $\text{P}\cdots\text{N}$ pnictogen bond and the $\text{O}-\text{H}_2\cdots\text{P}$ hydrogen bond

There is another factor which increases the stabilities of $\text{H}_2\text{XP}:\text{HNCHOH}$ complexes, and that is the enhancement of the electron-donating and electron-accepting abilities of the phosphorus in these complexes. Donation of a lone pair by N to P to form the pnictogen bond makes P a better electron-pair donor to O-H₂ to form the hydrogen bond, while electron donation by P to O-H₂ makes P a better electron-pair acceptor for the pnictogen bond. This cooperativity is supported by the charge-transfer energies reported in Table 3. The $\text{N}_{\text{lp}}\rightarrow\sigma^*\text{P}-\text{A}$ charge-transfer energy in a given $\text{H}_2\text{XP}:\text{HNCHOH}$ complex is always greater than it is in the corresponding $\text{H}_2\text{XP}:\text{HNNH}$ complex. Moreover, there is no back-donation from P to N₁-H₁ as these charge-transfer energies are less than 1 $\text{kJ}\cdot\text{mol}^{-1}$. The increased strength of the hydrogen bond is indicated by the $\text{P}_{\text{lp}}\rightarrow\sigma^*\text{H}_2-\text{O}$ charge-transfer energies, which are significantly greater than the $\text{P}_{\text{lp}}\rightarrow\sigma^*\text{H}_2-\text{N}_2$ energies of corresponding $\text{H}_2\text{XP}:\text{HNNH}$ and $\text{H}_2\text{XP}:\text{FNNH}$ complexes, even including $\text{H}_2(\text{CH}_3)\text{P}:\text{FNNH}$ and $\text{H}_3\text{P}:\text{FNNH}$ which are stabilized solely by $\text{N}_2-\text{H}_2\cdots\text{P}$ hydrogen bonds. In the three complexes $\text{H}_2\text{XP}:\text{HNCHOH}$ with the more electronegative substituents, the $\text{N}_{\text{lp}}\rightarrow\sigma^*\text{P}-\text{A}$ charge-transfer energies are greater than the $\text{P}_{\text{lp}}\rightarrow\sigma^*\text{H}_2-\text{O}$ energies, while in the three complexes with the more electropositive substituents, the $\text{P}_{\text{lp}}\rightarrow\sigma^*\text{H}_2-\text{O}$ charge-transfer energies are greater.

The presence of two BCPs in the molecular graphs of these complexes illustrated in Table S1 is another indication that these complexes are stabilized by both pnictogen bonds and hydrogen bonds. The $\text{P}\cdots\text{N}$ bond properties at BCPs reported in Table S3 for $\text{H}_2\text{XP}:\text{HNCHOH}$ complexes are similar to those of the $\text{H}_2\text{XP}:\text{HNNH}$ complexes, with ρ_{BCP} values between 0.010 and 0.034 au, positive values of $\nabla^2\rho_{\text{BCP}}$, and negative H_{BCP} for the complexes with X= F, Cl, NC and OH which have the shorter P-N distances. The $\text{O}-\text{H}_2\cdots\text{P}$ electron densities at BCPs are

greater than the BCP electron densities for $N_2-H_2 \cdots P$ hydrogen bonds. For the $O-H_2 \cdots P$ hydrogen bonds, $\nabla^2\rho_{BCP}$ values are positive and H_{BCP} values are negative except for $H_2(CN)P:HNCHOH$ and $H_2(NC)P:HNCHOH$.

The electron densities at bond critical points correlate exponentially with the corresponding distances across pnictogen and hydrogen bonds, in agreement with previous studies.^{34,35,36,37,38,39,40,41,42} As observed previously, the Laplacians for $P \cdots N$ pnictogen bonds tend to be positive for most interatomic distances, even for relatively short distances in bonds that have some covalent character.^{43,44,45} The variation of the energy densities with the P-N distance for $P \cdots N$ pnictogen bonds is illustrated in Fig. S1. Fig. S2 illustrates the energy density variation with the P-H₂ distance for hydrogen bonds.

Spin-Spin Coupling Constants

The PSO, DSO, FC, and SD components of the one-bond spin-spin coupling constants $^1J(P-N_1)$ across the $P \cdots N_1$ pnictogen bond are given in Table S3 of the Supporting Information. The two-bond coupling constants across the hydrogen bond, $^2hJ(N_2-P)$ for $H_2(CH_3)P:FNNH$ and $H_3P:FNNH$, and $^2hJ(O-P)$ for $H_2XP:HNCHOH$, can be found in Table S4. $J(N_2-P)$ values for complexes $H_2XP:HNNH$ and $H_2XP:FNNH$ are also given for comparison. The data of Tables S3 and S4 indicate that the Fermi-contact terms are very good approximations to total J values.

Coupling constants $^1J(P-N_1)$ across pnictogen bonds. Table 4 presents values of the spin-spin coupling constants $^1J(P-N_1)$ for coupling across the pnictogen bond. Excluding the complexes $H_2(CH_3)P:FNNH$ and $H_3P:FNNH$ which are not pnictogen bonded, $^1J(P-N_1)$ is always negative, and ranges from -8 Hz in $H_2(CH_3)P:HNNH$ to -59 Hz in $H_2CIP:HNCHOH$. For a fixed H_2XP , the absolute values of these coupling constants decrease in the order

$$HNCHOH > HNNH > FNNH$$

except for the complexes with H_2FP . Figure 5 presents plots of $^1J(P-N_1)$ versus the P-N₁ distance for these complexes. The second-order trendlines have correlation coefficients of 0.968, 0.968, and 0.953 for complexes with HNNH, FNNH, and HNCHOH, respectively.

Table 4. Spin-spin coupling constants (Hz) for complexes of H₂XP with HNNH, FNNH, and HNCHOH

Molecule:	HNNH	FNNH	HNCHOH	HNNH	FNNH	HNCHOH
H ₂ XP	¹ PJ(P-N ₁)	¹ PJ(P-N ₁)	¹ PJ(P-N ₁)	J(N ₂ -P)	J(N ₂ -P)	² hJ(O-P)
H ₂ FP	-55.8	-57.9	-52.3	-5.6	0.4	-17.9
H ₂ CIP	-55.9	-41.9	-58.5	-4.5	-0.1	-11.2
H ₂ (NC)P	-49.8	-47.3	-52.4	-4.0	0.4	-6.9
H ₂ (OH)P	-37.1	-21.6	-39.3	-5.0	-2.5	-19.1
H ₂ (CN)P	-30.9	-28.0	-36.7	-3.1	0.1	-4.8
H ₂ (CCH)P	-21.0	-8.7	-27.5	-4.3	-3.9	-14.0
H ₂ (CH ₃)P	-8.3	1.2	-15.9	-5.3	-18.0 ^a	-23.8
H ₃ P	-10.2	1.6	-16.8	-4.1	-12.1 ^a	-16.2

a) ²hJ(N₂-P) values for coupling across the N₂-H₂⋯P hydrogen bonds

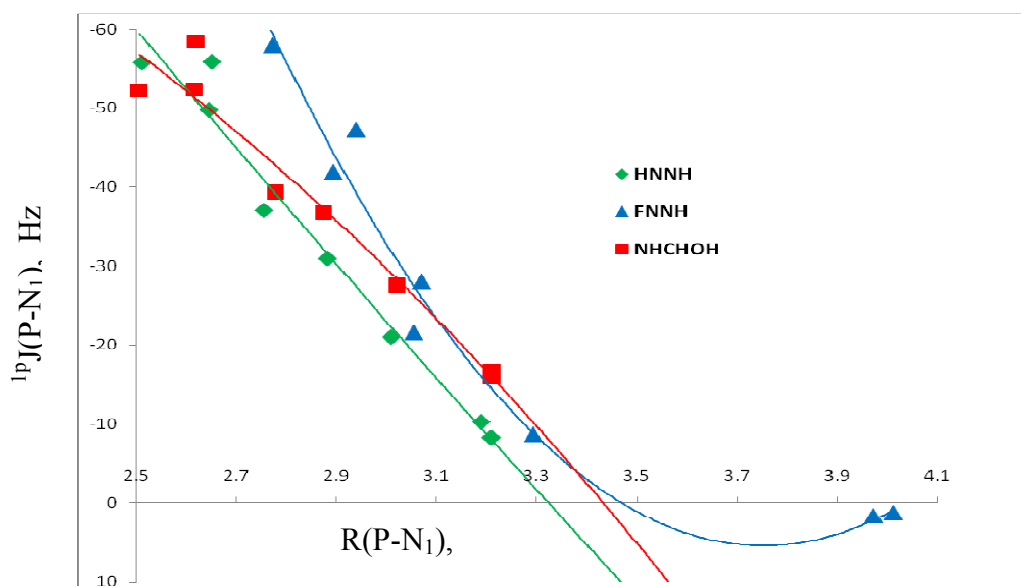


Fig. 5. ¹PJ(P-N₁) versus the P-N₁ distance for complexes of H₂XP with HNNH, FNNH, and HNCHOH

Coupling Constants ²hJ(Y₂-P) across Hydrogen Bonds. Coupling constants ²hJ(O-P) across the O-H₂⋯P hydrogen bonds in complexes H₂XP:HNCHOH are reported in Table 4. These range from -5 Hz in the complex with H₂(CN)P to -24 Hz in the complex with H₂(CH₃)P. Fig. S3 of the Supporting Information shows that the expected correlation between two-bond coupling constants across the hydrogen bond and the hydrogen bond distance is not found. There are two factors which undoubtedly influence the values of these coupling constants: the intermolecular O-P distance and the nonlinearity of the H₂-O-P hydrogen bond. Figure S3 indicates that H₂FP:HNCHOH and H₂(OH)P:HNCHOH have the two shortest O-P distances, and

they do have absolute values of ${}^2\text{h}J(\text{O-P})$ that are greater than the remaining complexes, except for $\text{H}_2(\text{CH}_3)\text{P}:\text{HNCHOH}$. This latter complex has an intermediate O-P distance, but a hydrogen bond that is linear. The fourth complex in the list of decreasing ${}^2\text{h}J(\text{O-P})$ is $\text{H}_3\text{P}:\text{HNCHOH}$, which has the next to longest O-P distance, but an H-O-P angle similar to that of $\text{H}_2(\text{CH}_3)\text{P}:\text{HNCHOH}$.

As noted above, $\text{H}_2(\text{CH}_3)\text{P}:\text{FNNH}$ and $\text{H}_3\text{P}:\text{FNNH}$ are stabilized solely by essentially linear $\text{N}_2\text{-H}_2\cdots\text{P}$ hydrogen bonds. ${}^2\text{h}J(\text{N}_2\text{-P})$ values for these two complexes are -18 and -12 Hz at $\text{N}_2\text{-P}$ distances of 3.559 and 3.615 Å, respectively. The remaining complexes in this series have absolute values of $J(\text{N}_2\text{-P})$ which are less than 4 Hz. Values of coupling constants $J(\text{N}_2\text{-P})$ vary between -3 and -6 Hz for complexes $\text{H}_2\text{XP}:\text{HNNH}$, and also show no correlation with the $\text{N}_2\text{-P}$ distance.

CONCLUSIONS

Ab initio MP2/aug²-cc-pVTZ calculations have been carried to investigate the properties of complexes formed between H_2XP , for $X = \text{F}, \text{Cl}, \text{NC}, \text{OH}, \text{CN}, \text{CCH}, \text{CH}_3$, and H , and the molecules HNNH , FNNH , and HNCHOH . These molecules can potentially act as both electron-pair donors to P to form pnictogen bonds, and electron-pair acceptors to form hydrogen bonds, thereby bridging the σ -hole and the lone pair of electrons at P . The results of these calculations support the following statements.

1. Complexes with HNNH and FNNH are stabilized by $\text{P}\cdots\text{N}_1$ pnictogen bonds, except for $\text{H}_2(\text{CH}_3)\text{P}:\text{FNNH}$ and $\text{H}_3\text{P}:\text{FNNH}$ which are stabilized solely by $\text{N}_2\text{-H}_2\cdots\text{P}$ hydrogen bonds. In the $\text{H}_2(\text{CCH})\text{P}:\text{FNNH}$ complex, the hydrogen bond makes a small contribution to stability. Complexes with HNCHOH are stabilized by $\text{P}\cdots\text{N}$ pnictogen bonds and nonlinear $\text{O-H}\cdots\text{P}$ hydrogen bonds. Thus, HNCHOH can bridge the σ -hole and the lone pair at P .
2. For a fixed base, binding energies of complexes decrease in the order $\text{HNCHOH} > \text{HNNH} > \text{FNNH}$, except for the binding energies of $\text{H}_2(\text{CH}_3)\text{P}$ and H_3P with HNNH and FNNH . Binding energies of complexes with HNCHOH and HNNH increase as the P-N_1 distance decreases, but binding energies of complexes with FNNH show little dependence on this distance.
3. The large binding energies of the complexes $\text{H}_2\text{XP}:\text{HNCHOH}$ are due to a cooperative effect involving the bonding at P . Electron-pair donation by N to P across the pnictogen bond makes

the P atom a better electron-pair donor for hydrogen bonding, while electron-donation by P across the hydrogen bond makes P a better electron-pair acceptor for pnictogen bonding.

4. Consistent with the dominant role of the pnictogen bond in stabilizing these complexes, the dominant charge-transfer interaction involves electron-pair donation by N across the pnictogen bond to the antibonding P-A orbital of H_2XP , with A the atom of X directly bonded to P. The only exceptions are found for $H_2(CH_3)P:HNNH$ and the complexes $H_2XP:FNNH$ and $H_2XP:HNCHOH$ with the more electropositive substituents CCH, CH_3 , and H. The dominant charge-transfer interaction for these is lone-pair donation by P across the hydrogen bond.

5. The molecular graphs for complexes show the existence of pnictogen bonds and hydrogen bonds. Values of electron densities at bond critical points correlate with the corresponding bond distances. Energy densities illustrate that the $P\cdots N$ bonds in some of these complexes have partial covalent character.

6. EOM-CCSD spin-spin coupling constants $^1J(P-N)$ across the pnictogen bond for each series of complexes correlate with the P-N distances. In contrast, $^2J(O-P)$ values across the $O-H\cdots P$ hydrogen bond for complexes $H_2XP:HNCHOH$ do not correlate with the O-P distance, most probably due to the nonlinearity of these bonds.

ACKNOWLEDGMENTS

This work was carried out with financial support from the Ministerio de Economía y Competitividad (Project No. CTQ201235513-C0202) and Comunidad Autónoma de Madrid (S2013/MIT2841, Fotocarbon). Thanks are also given to the Ohio Supercomputer Center and CTI (CSIC) for their continued computational support.

REFERENCES

- ¹ S. Scheiner, *J. Phys. Chem.*, 2011, **134**, 094315.
- ² S. Zahn, R. Frank, E. Hey-Hawkins, and B. Kirchner, *Chem. Eur. J.*, 2011, **17**, 6034–6038.
- ³ S. Scheiner, *Acc. Chem. Res.* 2012, **46**, 280–288.
- ⁴ S. Scheiner, *Int. J. Quantum Chem.*, 2013, **113**, 1609–1620.
- ⁵ J. E. Del Bene, I. Alkorta, and J. Elguero, The Pnictogen Bond in Review: Structures, Binding Energies, Bonding Properties, and Spin-Spin Coupling Constants of Complexes Stabilized by Pnictogen Bonds, in “Noncovalent Forces”, Vol. 19, “Challenges and Advances in Computational Chemistry and Physics”, Scheiner, S. Ed., Springer, 2015, pp. 191–263.

- 6 J. S. Murray, P. Lane, and P. Politzer, *Int. J. Quant. Chem.*, 2007, **107**, 2286–2292,
7 P. Politzer and J. S. Murray, A Unified View of Halogen Bonding, Hydrogen Bonding and
Other σ -Hole Interactions, in “Noncovalent Forces”, Vol. 19, “Challenges and Advances in
8 Computational Chemistry and Physics”, Scheiner, S. Ed., Springer, 2015, pp. 291-321.
9 J. E. Del Bene, I. Alkorta, G. Sánchez-Sanz, and J. Elguero, *J. Phys. Chem. A* 2013, **117**,
3133-3141.
10 U. Adhikari and S. Scheiner, *J. Chem. Phys.*, 2011, **135**, 184306.
11 I. Alkorta, J. Elguero, and J. E. Del Bene, *J. Phys. Chem. A* 2013, **117**, 4981-4987
12 J. A. Pople, J. S. Binkley, and R. Seeger, *Int. J. Quantum Chem.*, *Quantum Chem. Symp.*
13 1976, **10**, 1–19.
14 R. Krishnan and J. A. Pople, *Int. J. Quantum Chem.* 1978, **14**, 91–100.
15 R. J. Bartlett and D. M. Silver, *J. Chem. Phys.* 1975, **62**, 3258–3268.
16 R. J. Bartlett and G. D. Purvis, *Int. J. Quantum Chem.*, 1978, **14**, 561–581.
17 J. E. Del Bene, *J. Phys. Chem.*, 1993, **97**, 107–110.
18 T. H. Dunning, *J. Chem. Phys.*, 1989, **90**, 1007–1023.
D. E. Woon and T. H. Dunning, *J. Chem. Phys.* 1995, **103**, 4572–4585.
M. J. Frisch, G. W. Trucks, H. B. Schlegel, G. E. Scuseria, M. A. Robb, J. R. Cheeseman,
G. Scalmani, V. Barone, B. Mennucci, G. A. Petersson, H. Nakatsuji, M. Caricato, X. Li,
H. P. Hratchian, A. F. Izmaylov, J. Bloino, G. Zheng, J. L. Sonnenberg, M. Hada, M.
Ehara, K. Toyota, R. Fukuda, J. Hasegawa, M. Ishida, T. Nakajima, Y. Honda, O. Kitao, H.
Nakai, T. Vreven, J. A. Montgomery, J. E. Peralta, F. Ogliaro, M. Bearpark, J. J. Heyd, E.
Brothers, K. N. Kudin, V. N. Staroverov, R. Kobayashi, J. Normand, K. Raghavachari, A.
Rendell, J. C. Burant, S. S. Iyengar, J. Tomasi, M. Cossi, N. Rega, N. J. Millam, M. Klene,
J. E. Knox, J. B. Cross, V. Bakken, C. Adamo, J. Jaramillo, R. Gomperts, R. E. Stratmann,
O. Yazyev, A. J. Austin, R. Cammi, C. Pomelli, J. W. Ochterski, R. L. Martin, K.
Morokuma, V. G. Zakrzewski, G. A. Voth, P. Salvador, J. J. Dannenberg, S. Dapprich, A.
D. Daniels, O. Farkas, J. B. Foresman, J. V. Ortiz, J. Cioslowski and D. J. Fox, Gaussian,
Inc., Wallingford CT, 2009.
19 R. F. W. Bader, *Chem. Rev.* 1991, **91**, 893–928.
20 R. F. W. Bader, *Atoms in Molecules, A Quantum Theory*; Oxford University Press, Oxford,
1990.
21 P. L. A. Popelier, *Atoms In Molecules. An Introduction*, Prentice Hall, Harlow, England,
2000.
22 C. F. Matta and R. J. Boyd *The Quantum Theory of Atoms in Molecules: From Solid State
to DNA and Drug Design*, Wiley-VCH, Weinham, 2007.
23 T. A. Keith, AIMAll (Version 11.08.23), TK Gristmill Software, Overland Park KS, USA,
2011 (aim.tkgristmill.com).
24 I. Rozas, I. Alkorta, and J. Elguero, *J. Am. Chem. Soc.*, 2000, **122**, 11154–11161.
25 A. E. Reed, L. A. Curtiss, and F. Weinhold, *Chem. Rev.* 1988, **88**, 899–926.
26 E. D. Glendening, J. K. Badenhoop, A. E. Reed, J. E. Carpenter, J. A. Bohmann, C. M.
Morales, C. R. Landis, and F. Weinhold, NBO 6.0; University of Wisconsin: Madison, WI,
2013.
27 A. D. Becke, *J. Chem. Phys.*, 1993, **98**, 5648–5652.
28 C. Lee, W. Yang, and R. G. Parr, *Phys. Rev. B* 1988, **37**, 785–789.
29 S. A. Perera, M. Nooijen, and R. J. Bartlett, *J. Chem. Phys.* 1996, **104**, 3290–3305.

- 30 S. A. Perera, H. Sekino, and R. J. Bartlett, *J. Chem. Phys.* 1994, **101**, 2186–2196.
31 A. Schäfer, H. Horn, and R. Ahlrichs, *J. Chem. Phys.* 1992, **97**, 2571–2577.
32 ACES II is a program product of the Quantum Theory Project, University of Florida.
Authors: J. F. Stanton, J. Gauss, J. D. Watts, M. Nooijen, N. Oliphant, S. A. Perera, P. G.
Szalay, W. J. Lauderdale, S. R. Gwaltney, S. Beck, A. Balkova, E. D. Bernholdt, K.-K.
Baeck, P. Tozyczko, H. Sekino, C. Huber and R. J. Bartlett, Integral packages included are
VMOL (J. Almlöf and P. R. Taylor), VPROPS (P. R. Taylor), ABACUS (T. Helgaker, H.
J. A. Jensen, P. Jorgensen, J. Olsen and P. R. Taylor). Brillouin–Wigner perturbation
theory was implemented by J. Pittner.
- 33 J. E. Del Bene, I. Alkorta, and J. Elguero, *J. Phys. Chem. A* 2013, **117**, 6893–6903.
34 O. Knop, R. J. Boyd, and S. C. Choi, *J. Am. Chem. Soc.* 1988, **110**, 7299–7301.
35 G. V. Gibbs, F. C. Hill, M. B. Boisen, and R. T. Downs, *Phys. Chem. Minerals* 1998, **25**,
585–590.
- 36 I. Alkorta, L. Barrios, I. Rozas, and J. Elguero, *J. Mol. Struct. Theochem* 2000, **496**, 131–
137.
- 37 O. Knop, K. N. Rankin, and R. J. Boyd, *J. Phys. Chem. A* 2001, **105**, 6552–6566.
38 O. Knop, K. N. Rankin, and R. J. Boyd *J. Phys. Chem. A* 2003, **107**, 272–284.
39 E. Espinosa, I. Alkorta, J. Elguero, and E. Molins, *J. Chem. Phys.* 2002, **117**, 5529–5542.
40 I. Alkorta and J. Elguero, *Struct. Chem.* 2004, **15**, 117–120.
41 T. H. Tang, E. Deretey, S. J. K. Jensen, and I. G. Csizmadia, *Eur. Phys. J. D.*, 2006, **37**,
217–222.
- 42 I. Mata, I. Alkorta, E. Molins, and E. Espinosa, *Chem. Eur. J.* 2010, **16**, 2442–2452.
43 J. E. Del Bene, I. Alkorta, and J. Elguero, *J. Phys. Chem. A* 2014, **118**, 10144–10154.
44 J. E. Del Bene, I. Alkorta, and J. Elguero, *J. Phys. Chem. A* 2015, **119**, 3125–3133.
45 J. E. Del Bene, I. Alkorta, and J. Elguero, *J. Phys. Chem. A* 2015, **119**, 5853–5864.